# **INSTRUMENT PERFORMANCE AND CALIBRATION OF AMSR-E AND AMSR2**

K. Imaoka<sup>a, \*</sup>, M. Kachi<sup>a</sup>, M. Kasahara<sup>a</sup>, N. Ito<sup>a</sup>, K. Nakagawa<sup>a</sup>, and T. Oki<sup>b</sup>

<sup>a</sup> Japan Aerospace Exploration Agency, Tsukuba, Japan - imaoka.keiji@jaxa.jp <sup>b</sup> Institute of Industrial Science, The University of Tokyo, Tokyo, Japan - taikan@iis.u-tokyo.ac.jp

KEY WORDS: Climate change, Remote sensing, Microwave radiometer

#### **ABSTRACT:**

The Global Change Observation Mission (GCOM) consists of two satellite observing systems and three generations to achieve global, comprehensive, and long-term Earth monitoring. The first satellite of the GCOM-W (Water) series will be GCOM-W1 with the Advanced Microwave Scanning Radiometer-2 (AMSR2) onboard. AMSR2 is a successor of AMSR on the Advanced Earth Observing Satellite-II (ADEOS-II) and AMSR for EOS (AMSR-E) on NASA's Aqua satellite. Basic performance of AMSR2 will be similar to that of AMSR-E based on the minimum requirement of data continuity of AMSR-E, with several enhancements including larger main reflector (2.0 m), additional channels in C-band receiver, and improved calibration system. AMSR-E was launched in 2002 and is still gathering global brightness temperatures for more than eight years beyond its scheduled operational period of three years. Despite the warm-load calibration issue, the instrument indicates good performance in long-term stability. Based on the AMSR and AMSR-E experience, several design changes were made for the AMSR2 warm load, including changes in thermal stabilization and solar light shielding. Pre-launch testing is being performed, such as antenna pattern and detector nonlinearity measurements. The testing results will be reflected in sensor calibration model. After the launch, a deep-space calibration maneuver will be performed just one time during the initial checkout period to check consistency between main reflector and cold sky mirror, as well as to see scan biases for cold brightness temperatures. Further post-launch calibration activities will be performed, including cross calibration among similar microwave radiometers. Since GCOM-W1 will join the A-Train constellation, cross calibration between AMSR-E and AMSR2 will be very simple and thus accurate. Continuation from AMSR-E to AMSR2 with the consistent cross calibration will enable us to construct over 20-years data set of unique geophysical parameters including all-weather sea surface temperatures and soil moisture content. Current target launch year of GCOM-W1 is in Japanese fiscal year 2011.

#### 1. INTRODUCTION

Microwave radiometers have clear advantages in measuring geophysical parameters related to water over the Earth. Therefore, they have been playing an important role in observing various phases of water, such as water vapour, cloud liquid water, precipitation, sea ice, and snow for a long time, such as by the Special Sensor Microwave/Imager (SSM/I) onboard multiple generations of the Defence Meteorological Satellite Program (DMSP). The Microwave Scanning Radiometer (MSR) was the first Japanese experience to develop, launch, and operate such microwave radiometers. As a successor to MSR, the Advanced Microwave Scanning Radiometer (AMSR) was developed for the Advanced Earth Observing Satellite-II (ADEOS-II or Midori-II) by the Japan Aerospace Exploration Agency (JAXA), which was the National Space Development Agency of Japan (NASDA) at that time. There were many engineering challenges in developing AMSR instrument, in terms of number of channels, spatial resolution, global observing capability and so forth. Also, the AMSR for the Earth Observing System (AMSR-E), which was a sister instrument of AMSR, was developed and provided by JAXA for the EOS Aqua satellite (Kawanishi et al., 2003). Unfortunately, the AMSR instrument was lost due to the satellite malfunction in October 2003. Approximately seven month's of data were obtained, with the valuable synchronous observations by other onboard instruments such as the Global Imager (GLI) and SeaWinds, which was the NASA's ocean scatterometer. The AMSR-E instrument has been successfully

accumulating the data for more than eight (8) years. The first satellite of the Global Change Observation Mission (GCOM) will be GCOM-W1, which is the first generation of GCOM-W (Water) series. The AMSR2 instrument will be the sole instrument onboard.

#### 2. INSTRUMENTS

## 2.1 AMSR and AMSR-E

AMSR is a eight-frequency, total-power microwave radiometer system with dual polarization capability for all frequency bands, except the 50.3 and 52.8GHz channels. The frequency bands range from 6.9GHz to 89.0GHz. Mapping of the Earth's surface is performed by conically scanning the sensor system at 40 rpm with a constant incidence angle of 55 degrees. A feed-horn cluster is placed around the focal plane to realize the multifrequency measurement. Typical calibration method was adopted for this type of microwave radiometer: external twopoints calibration by using the high temperature noise source (HTS, a hot load calibration target) and the cold-sky mirror (CSM) which introduces the deep sky temperature to feed horns. The 2.0m diameter offset parabolic antenna was the largest spaceborne microwave radiometer antenna of its kind.

AMSR-E was developed based on the AMSR design, with some modifications to accommodate the instrument within the Aqua's satellite resources. Major changes include smaller main reflector with 1.6m diameter, excluding the 50.3 and 52.8GHz

<sup>\*</sup> Corresponding author. K. Imaoka. Japan Aerospace Exploration Agency, Tsukuba, Japan - imaoka.keiji@jaxa.jp

channels, and addition of the Orbital Balancing Mechanism (OBM), which is to minimize the disturbances by AMSR-E rotation. Thanks to the lower orbit altitude of Aqua, the spatial resolution is not so degraded even with the smaller antenna. Also, the Advanced Microwave Sounding Unit (AMSU) has several channels around 50-60GHz. Major performance and characteristics of both instruments are summarized in Table 1.

Table 1. AMSR and AMSR-E characteristics and performance

Center	Band	3dB Beam	Ground IFOV	ΝΕΔΤ	
Freq.	Width	Width	Scan x along track	@150	
_		AMSR/AMSR-E	AMSR/AMSR-E	ĸ	
(GHz)	(MHz)	(deg)	(km)		
				(K)	
6.925	350	1.8 / 2.2	40x70 / 43x75	0.34	
10.65	100	1.2 / 1.5	27x46 / 29x51	0.7	
18.7	200	0.65 / 0.8	14x25 / 16x27	0.7	
23.8	400	0.75 / 0.92	17x29 / 18x32	0.6	
36.5	1000	0.35 / 0.42	8x14 / 8x14	0.7	
50.3	200	0.25 / -	6x10 / -	1.8	
52.8	400	0.25 / -	6x10 / -	1.6	
89.0A	3000	0.15 / 0.19	3x6 / 4x7	1.2	
89.0B	3000	0.15 / 0.19	3x6 / 4x6	1.2	
Antenna		Offset parabolic antenna; effective aperture size			
		2.0 m for AMSR, 1.6 m for AMSR-E			
Polarization		Vertical and Horizontal (only Vertical for 50-GHz			
		band)			
Sampling interval,		AMSR: 10x10km (5x5 km for 89GHz)			
Scan x along track		AMSR-E: 9x10km (4.5x4 km for 89GHz A $\rightarrow$ B,			
		4.5x6 km for 89GHz B→A)			
Incidence angle		55 degrees (54.5 degrees for 89B)			
Dynamic range		2.7 - 340 K			
Swath width		AMSR: 1600 km, AMSR-E: 1450 km			
Integration time		2.5 msec (1.2 msec for 89GHz)			
Quantization		10 bit (12 bit for 6.925 GHz)			
Scan rate	e	40 rpm (1.5sec per scan)			

## 2.2 AMSR2

AMSR2 will succeed most of the characteristics of AMSR-E, with some important improvements. Major changes from AMSR-E include the larger main reflector with 2.0m diameter, addition of 7.3GHz channels, 12bit quantization for all channels, and improvements in calibration system. AMSR2 channel characteristics are shown in Table 2 and instrument overview in Figure 1. One of the most critical issue of the AMSR and AMSR-E instruments was the physical temperature nonuniformity over the microwave absorber of the HTS and its variation in orbit. This issue made their calibration nonstraightforward. Thermal design changes were applied to AMSR2 to improve this situation. Also, intensive sunlight shielding is applied to avoid calibration uncertainties due to the sunlight intrusion over the load. Figure 2 shows an example of HTS testing in thermal-vacuum environment.

Table 2. AMSR2 characteristics and performance

Center Freq. (GHz)	Band Width (MHz)	Beam Width (3dB, deg)	Ground IFOV (scan x along track, km)	Sampling Interval (km)
6.925/ 7.3	350	1.8	35 x 62	
10.65	100	1.2	24 x 42	10
18.7	200	0.65	14 x 22	10
23.8	400	0.75	15 x 26	
36.5	1000	0.35	7 x 12	
89.0	3000	0.15	3 x 5	5

In the brightness temperatures at 6.9GHz frequency channels of AMSR and AMSR-E, we have observed intensive radiofrequency interference (RFI) signals, particularly over land areas. Due to this situation, the 6.9GHz channels can not be utilized in the current retrieval algorithm to estimate global soil moisture content, despite its most plausible performance among the AMSR-E channels for estimating under vegetation cover. To increase the information to identify the RFI signals, new dual-polarization channels in 7.3GHz frequency band will be added to AMSR2. Although having more sub-bands is ideal to identify and remove the RFI signals, only one sub-band will be added due to the limitation of instrument's resources. By using the different responses to RFI at 6.9 and 7.3GHz bands, we expect to increase the information to distinguish RFI-contaminated footprints.

The 2.0m diameter main reflector, compared to the 1.6m diameter of AMSR-E, will improve the spatial resolution. Although the main reflector of AMSR was 2.0m in diameter, it was a fixed-type antenna without deployable mechanism.

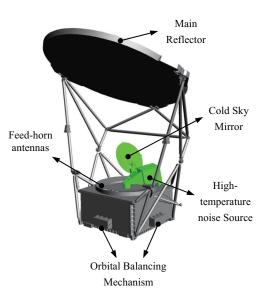


Figure 1. Overview of AMSR2 instrument

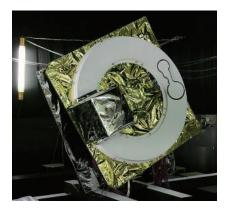


Figure 2. Photo showing solar heating test of HTS under thermal-vacuum environment

### 3. CALIBRATION

Calibrating instruments is the crucial issue in performing longterm monitoring of climate and environment, as well as the daily use in operational agencies such as the numerical weather forecasting. For the long-term monitoring, stable calibration without any drifts is a key to detect proper trends of climate. Calibration consistency among similar instruments is a bottom for generating merged dataset. The calibration, in the broad sense, covers various activities including careful design of the instruments, pre-flight laboratory calibration testing, evaluation and correction of the onboard calibration, validation of brightness temperatures using ground targets, and crosscalibration with similar instruments. The activities those have done for AMSR and AMSR-E so far, and have been implemented and/or planned for AMSR2 will be described as follows.

# 3.1 AMSR-E and AMSR

Due to the HTS issue mentioned in the previous section, some specific correction procedures have been added in computing AMSR and AMSR-E brightness temperatures (Imaoka et al., 2003). First step is to express the HTS effective temperature (not just the physical temperature) by empirically combining eight platinum resistance thermometer (PRT) readings. Based on this "first guess" of orbital changes of HTS effective temperature, we then compute the final values by utilizing the relationship between receiver physical temperature and its gain variation. Also, we have made some empirical corrections for possible non-linearity of receivers. In doing these corrections, we have relied on the cross calibration with similar instruments including SSM/I and the Tropical Rainfall Measuring Mission (TRMM) Microwave Imager (TMI), and comparison with simulated brightness temperatures based on separately generated geophysical fields from other data sources such as sea surface temperature. There is still a room for improvement in the current calibration. We expect to update the AMSR-E calibration, in synchronizing the cross calibration with AMSR2 data.

Calibration stability of microwave radiometers is highly affected by the physical temperatures of the instrument. As shown in Figure 3, physical temperatures at eight PRT positions (from top to bottom in Figure 3) over HTS indicate consistent increasing trend in the maximum temperatures. This might be due to the aging of the multi-layer insulation (MLI) materials, which typically increases the sunlight absorption during the daytime. We keep monitoring the brightness temperature trends over some specific regions and over oceans, to see if this type of instrument changes can affect the calibration stability.

# 3.2 AMSR2

As stated earlier, the AMSR2 instrument will employ the improved thermal design for HTS. Therefore, we are expecting that the simple two-point calibration will work for AMSR2. Considering the characteristics of the AMSR2 detectors, the receiver non-linearity is one of the largest error sources in computing brightness temperatures, particularly for the lower frequency channels which use wider area of detector dynamic range. For the AMSR2 instrument, we have been measuring detailed input-output characteristics of the detectors. Using these measurement results, we will correct non-linearity.

During the initial checkout phase, a deep space calibration maneuver will be conducted to check the consistency of emissivity between main reflector and cold-sky mirror, scan bias errors for cold observation target, and so forth. This type of deep space calibration has been tested for TMI (Wentz, et al., 2001) and WindSat (Jones et al., 2006), which is the polarimetric microwave radiometer onboard the Coriolis satellite. Also, limited analysis was performed for AMSR-E to utilize the deep space measurement opportunity during the MODIS lunar calibration maneuver (Arai et al., 2005). The deep space calibration will be implemented by an single orbit inertia-lock maneuver over open ocean areas.

Although it was not described in the AMSR-E section of this article, confirmation and correction of geolocation errors will be performed by the same methodology that used for AMSR-E and AMSR. By minimizing the geolocation errors at predetermined test areas, where the brightness temperature contrast is clear such as around islands and coastlines, angular offsets of instrument alignment will be determined.

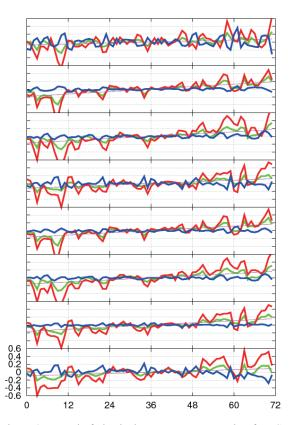


Figure 3. Trend of physical temperature anomaly of HTS. Red, green, and blue lines indicate trends of maximum, average, and minimum temperatures during a orbit. Vertical and horizontal axes indicate temperature anomaly [K] and months from the beginning, respectively.

#### 3.3 Cross-Calibration activities

Although cross-calibrating the similar instruments has been a pre-existing concept and implemented for many sensors, it is recently becoming a common concern for many people with the increase of the number of the Earth observing instruments. Several cross-calibration initiatives are now emerging in the international community to deal with this issue. One of the important concepts of the GCOM mission is to construct continuous data records by cross-calibrating the consecutive generation instruments with using the at least oneyear overlap in observing period. Also, the continuity from AMSR-E to AMSR2 is highly desired. The GCOM-W1 satellite will join in the A-Train satellite constellation (Stephens et al., 2002) to assure this continuity. The position of GCOM-W1 will be just ahead of the Aqua satellite. Therefore, cross-calibrating AMSR2 and AMSR-E will be very simple with nearly the simultaneous observation by the almost identical sensor specifications, and thus accurate without any assumptions.

Cross calibration among various instruments with somewhat different sensor characteristics and observing local times is more complicated. One idea for cross-calibrating the multiple polar-orbiting satellites with different observing local time is to use a non-sun-synchronous satellite which can cover various observing local time by its precession orbit. Currently, the TMI instrument can be used for this purpose, although the calibration of TMI itself should be first improved (e.g., Gopalan et al., 2009). The same concept will be applicable to the Global Precipitation Measurement (GPM) and the cross calibration working group is now pursuing the appropriate methodology.

#### 4. SUMMARY

We have described and summarized the instrument performance and calibration of AMSR, AMSR-E, and AMSR2. AMSR2 will be improved based on the experiences in AMSR and AMSR-E activities, while the AMSR-E data records will be re-calibrated and reprocessed based on the cross calibration with improved AMSR2 data. Combining the AMSR-E and multiple generation of GCOM-W series, we will be able to obtain long-term microwave brightness temperature data record over 20-years. Also by integrating with the historical data records beginning from the Scanning Multifrequency Microwave Radiometer (SMMR) and SSM/I, some snapshots of climate variability must be observed such as the trend in sea ice extent by the over 50-years dataset.

#### References

Arai, Y., T. Mutoh, K. Imaoka, Y. Fujimoto, and A. Shibata, 2005. Investigation of radio frequency interference over Japan using AMSR and AMSR-E data. *Proc. IGARSS*, 5, pp. 3445-3447.

Gopalan, K., W.L. Jones, S. Biswas, S. Bilanow, T. Wilheit, and T. Kasparis, 2009. A time-varying radiometric bias correction for the TRMM Microwave Imager. *IEEE Trans. Geosci. Remote Sens.*, 47(11), pp. 3722-3730.

Imaoka, K., Y. Fujimoto, M. Kachi, T. Takeshima, K. Shiomi, H. Mikai, T. Mutoh, M. Yoshikawa, and A. Shibata, 2003. Postlaunch calibration and data evaluation of AMSR-E. *Proc. IGARSS*, pp. 666 -668.

Jones, W.L., J.D. Park, S. Soisuvarn, L. Hong, P.W. Gaiser, and K.M. St. Germain, 2006. Deep-space calibration of the WindSat radiometer. *IEEE Trans. Geosci. Remote Sens.*, 44(3), pp. 476-495.

Kawanishi, T., T. Sezai, Y. Ito, K. Imaoka, T. Takeshima, Y. Ishido, A. Shibata, M. Miura, H. Inahata, and R. W. Spencer,

2003. The Advanced Microwave Scanning Radiometer for the Earth Observing System (AMSR-E), NASDA's contribution to the EOS for global energy and water cycle studies. *IEEE Trans. Geosci. Remote Sens.*, 41(2), pp. 184-194.

Stephens, G.L., D.G. Vane, R.J. Boain, G.G. Mace, K. Sassen, Z. Wang, A.J. Illingworth, E.J. O'Connor, W.B. Rossow, S.L. Durden, S.D. Miller, R.T. Austin, A. Benedetti, C. Mitrescu, and The CloudSat Science Team, 2002. The CloudSat mission and the A-Train. *Bull. Amer. Meteor. Soc.*, 83(12), pp. 1771-1790.

Wentz, F.J., P. Ashcroft, and C. Gentemann, 2001. Post-launch calibration of the TRMM Microwave Imager. *IEEE Trans. Geosci. Remote Sens.*, 39(2), pp. 415-422.